Cellular/Molecular

Opposite Regulation of Slick and Slack K^+ Channels by Neuromodulators

Celia M. Santi,[1]* Gonzalo Ferreira,[1,3]* Bo Yang,[4]* Valeswara-Rao Gazula,[4] Alice Butler,[1] Aguan Wei,[1] Leonard K. Kaczmarek,[4] and Lawrence Salkoff[1,2]

Departments of [1]Anatomy and Neurobiology and [2]Genetics, Washington University School of Medicine, St. Louis, Missouri 63110, [3]Departamento de Biofisica, Universidad de la República, Facultad de Medicina, 11800 Montevideo, Uruguay, and [4]Department of Pharmacology, Yale University School of Medicine, New Haven, Connecticut 06520

Slick (Slo2.1) and Slack (Slo2.2) are two novel members of the mammalian *Slo* potassium channel gene family that may contribute to the resting potentials of cells and control their basal level of excitability. Slo2 channels have sensors that couple channel activity to the intracellular concentrations of Na^+ and Cl^- ions (Yuan et al., 2003). We now report that activity of both Slo2 channels is controlled by neuromodulators through $G\alpha_q$-protein coupled receptors (GqPCRs) (the M_1 muscarinic receptor and the mGluR1 metabotropic glutamate receptor). Experiments coexpressing channels and receptors in *Xenopus* oocytes show that Slo2.1 and Slo2.2 channels are modulated in opposite ways: Slo2.1 is strongly inhibited, whereas Slo2.2 currents are strongly activated through GqPCR stimulation. Differential regulation involves protein kinase C (PKC); application of the PKC activator PMA, to cells expressing channels but not receptors, inhibits Slo2.1 whole-cell currents and increases Slo2.2 currents. Synthesis of a chimera showed that the distal carboxyl region of Slo2.1 controls the sensitivity of Slo2.1 to PMA. Slo2 channels have widespread expression in brain (Bhattacharjee et al., 2002, 2005). Using immunocytochemical techniques, we show coexpression of Slo2 channels with the GqPCRs in cortical and hippocampal brain sections and in cultured hippocampal neurons. The differential control of these novel channels by neurotransmitters may elicit long-lasting increases or decreases in neuronal excitability and, because of their widespread distribution, may provide a mechanism to activate or repress electrical activity in many systems of the brain.

Key words: **sodium-activated potassium channels; Slo channels; BK channels; Slick; Slack; PKC phosphorylation; $G\alpha_q$-coupled receptors; modulation by neurotransmitters**

Introduction

In pioneering studies on the cellular basis of learning in *Aplysia*, Eric Kandel called attention to the importance of a subtype of potassium channels modified by neuromodulators. This class of potassium channels may elicit a persistent change in neuronal excitability, lasting longer than that which can be achieved by voltage-dependent channels alone (Klein et al., 1982; Hochner and Kandel, 1992). The extent to which these modulated potassium conductances participate in controlling basal neuronal excitability is currently the subject of investigation in many systems.

Received Aug. 10, 2005; revised April 3, 2006; accepted April 3, 2006.

This work was supported by National Institutes of Health Grants R24 RR017342-01 and R01 GM067154-01A1 (L.S.) and DC-01919 and NS42202 (L.K.K.). B.Y. is supported by a Heritage Affiliate Postdoctoral Fellowship from the American Heart Association. G.F. acknowledges the support of Universidad de la Republica (Uruguay), Centro de Estudios Científicos de Santiago (Chile), and Third World Academy of Sciences. A.W. was supported by National Science Foundation Grant IBN-0117341. We thank Jonathan Garst Orozco and Marisa Jackson for isolating *Xenopus Laevis* oocytes and Berevan Bevan, Gloria Fawcett, Karen Lawrence, Josephine Garcia-Ferrer, Walter Boyle, Mike Nonet, Arthur Loewy, and David Gottlieb for their support. We also thank Pato Rojas for his helpful comments. We thank N. Gautam for the M_1 receptor cDNA, Lakshmi Pulakat for the angiotensin type IB receptor, and S. Nakanishi for the mGluR1 receptor. We thank Dr. Fred J. Sigworth and Yangyang Yan for providing us the stable Slack-expressing HEK cell line.

*C.M.S., G.F., and B.Y. contributed equally to this work.

Correspondence should be addressed to Lawrence Salkoff, Department of Anatomy and Neurobiology, Washington University School of Medicine, 660 South Euclid Avenue, St. Louis, MO 63110. E-mail: salkoffl@pcg.wustl.edu.

DOI:10.1523/JNEUROSCI.3372-05.2006

 0270-6474/06/265059-10$15.00/0

Currently, the best characterized potassium channels that are modulated by neurotransmitters are the KCNQ channels, which carry the M-current (Brown and Adams, 1980; Cooper and Jan, 2003), and G-protein-gated inwardly rectifying K^+ channels, which directly interact with G-proteins (Luscher et al., 1997; Mao et al., 2004). Other reports suggest that four transmembrane K^+ channels (Lesage et al., 2000; Talley et al., 2000; Bockenhauer et al., 2001; Lei et al., 2001; Chemin et al., 2003; Heurteaux et al., 2004), and even voltage-dependent potassium channels (Johnston et al., 2003), are modulated by neurotransmitters. Here we demonstrate the differential modulation by neuromodulators of two closely related potassium channels, Slo2.1 and Slo2.2, by functional coexpression of these channels and $G\alpha_q$-protein coupled receptors (GqPCRs) in a heterologous system. Using immunohistochemical techniques, we also demonstrate that these channels and GqPCRs (the M_1 muscarinic receptor and the mGluR1 metabotropic glutamate receptor) are coexpressed in the same neurons in several regions of the brain. Slo2 channels are members of the high-conductance Slo family of potassium channels. Unlike Slo1 BK high-conductance channels that are sensitive to both voltage and intracellular calcium (Atkinson et al., 1991; Adelman et al., 1992; Butler et al., 1993; Tseng-Crank et al., 1994), Slo2 channels have very low voltage sensitivity and are activated by intracellular Na^+ and Cl^- rather than Ca^{2+}. Indeed,

although they belong to the large family of potassium channels that contain six transmembrane domains per subunit, Slo2.1 and Slo2.2 lack the canonical arrangement of gating charges found in S4, which are associated with voltage-dependent gating in all other family members.

Sodium-activated potassium channels were originally identified in cardiomyocytes in which they may provide protection against ischemia, which is accompanied by an increase in intracellular sodium (Kameyama et al., 1984; Luk and Carmeliet, 1990). However, they were also discovered in neurons (Dryer et al., 1989) and may play a role during normal electrical activity (Dryer, 1994). In the laboratory, these channels are usually studied under conditions of high intracellular Na^+, but they are also significantly active at normal Na^+ and Cl^- concentrations (Bhattacharjee et al., 2002, 2003; Yuan et al., 2003). In this paper, we show that Slo2.2 channels are activated by neuromodulators, whereas Slo2.1 channels are inhibited by neuromodulators acting through GqPCRs; we also show that Slo2 channels and GqPCRs are coexpressed in the same cell types in many regions of the brain. Furthermore, we show that both Slo2 channels and GqPCR receptors are coexpressed in the cell soma and adjacent areas in which they may modulate spatial integration and action potential generation.

Materials and Methods

Xenopus *oocyte expression.* To obtain efficient expression of *Slo2.1* (human) and *Slo2.2* (rat) cDNAs and chimeric constructs, in *Xenopus* oocytes, we used pOX, a vector we optimized for oocyte expression. The chimera C1 was constructed by joining the Slo2.2 core to the Slo2.1 tail at a conserved *Stu*I site at residue 380 (Slo2.2) and residue 433 (Slo2.1). The arrows in Figures 1 and 4*a* indicate the site of ligation. The M_1 receptor, angiotensin receptor type IB (AT1B), and mGluR1 were also subcloned into pOX. Capped cRNA was synthesized using the T3 mMessage mMachine kit (Ambion, Austin, TX). *Slo2.2* was linearized using *Not*I. cRNA reactions were resuspended in nuclease-free water to a final concentration of 1.5 μg/μl. Oocytes were harvested from adult female *Xenopus laevis* as described previously (Yuan et al., 2000). Defolliculated oocytes were injected with ~75 ng of cRNA using a Drummond Scientific (Broomall, PA) nanoinjector. Injected oocytes were incubated at 18°C in ND96 medium (in mM): 96 NaCl, 2 KCl, 1.8 $CaCl_2$, 1 $MgCl_2$, and 5 HEPES, pH 7.5 with NaOH. Oocytes were electrophysiologically analyzed 3–5 d after injection.

Electrophysiology: Xenopus *oocytes.* Two-microelectrode voltage-clamp recordings were obtained in ND96 plus 1–2 mM DIDS to block the endogenous chloride conductances. Phorbol 12-myristate 13-acetate (PMA) or receptor agonists were applied to the recording chamber either directly or by continuous perfusion. For patch-clamp experiments, before recording, the vitelline membranes were mechanically removed. Cell-attached recordings were done with ND96 in the bath and with a pipette solution containing the following (in mM): 80 K-gluconate, 80 Na-gluconate, 5 HEPES, and 2 $MgCl_2$, pH 7.2 with KOH. Inside-out patches were obtained perfusing the intracellular side of the membrane with high Na-Cl solution containing the following (in mM): 80 KCl, 80 NaCl, 5 HEPES, and 5 EGTA, pH 7.2 with KOH. In the experiments with 0 Na, NaCl was substituted by choline-Cl. In experiments performed with low Na and low Cl^- solution, the bath contained the following (in mM): 20 NaCl, 20 KCl, 60 K-gluconate, 5 HEPES, and 5 EGTA. The pipette solution was the same as the one described above for cell-attached recordings. Pipette tip resistance ranged from 3 to 5 MΩ. Traces were acquired using an Axopatch 200A (Molecular Devices, Palo Alto, CA), digitized at 10 kHz, and filtered at 2 kHz. Data were analyzed using pClamp 9 (Molecular Devices), SigmaPlot 5 (Jandel Scientific, Corte Madera, CA) or Origin 6.0 (Microcal Software, Northampton, MA). Drugs and pharmacological agents used in this study were purchased from Sigma (St. Louis, MO).

*Transient transfected HEK cells expressing the Slick (*Slo 2.1*) channel.* The Slick pCDNA3 construct, containing the full-length wild-type *Slo2.1* sequence, was used to transfect HEK-293 cells. Transient transfection was performed using Lipofectamine 2000 (Invitrogen, Carlsbad, CA). These HEK cells were cultured in DMEM supplemented with 10% fetal bovine serum and penicillin–streptomycin (Invitrogen).

*Stable cell line expressing the Slack (*Slo 2.2*) channel.* The Slack-HA.pCDNA3 construct, containing the full-length wild-type *Slo2.2* sequence, was used to transfect HEK-293 cells. Transfection was performed using the SuperFect Transfection Reagent (Qiagen, Valencia, CA). The stable Slack-expressing HEK cell line was confirmed by patch-clamp recordings and Western blot. These HEK cells were cultured in a modified low-sodium DMEM supplemented with 10% fetal bovine serum and penicillin–streptomycin (Invitrogen).

Electrophysiology: cells expressing Slick or Slack channels. Nystatin perforated patch-clamp recordings from Slick- or Slack-expressing HEK-293 cells were obtained at room temperature (21–23°C) using the gigaseal patch-clamp technique (Hamill et al., 1981). Electrodes of 3–5 MΩ resistance were pulled from TW150F-6 micropipettes (World Precision Instruments, Sarasota, FL) on a horizontal Flaming/Brown micropipette puller (model P-87; Sutter Instruments, Novato, CA), fire-polished, coated with dental wax, and filled with appropriate filling solutions.

Cells were bathed in a solution containing the following (in mM): 140 NaCl, 1 $CaCl_2$, 5 KCl, 29 glucose, and 25 HEPES, pH 7.4. The pipette solution contained the following (in mM): 100 K-gluconate, 30 KCl, 5 Na-gluconate, 29 glucose, 5 EGTA [2 Na_2ATP, 0.2 GTP (for Slack recordings)], and 10 HEPES, pH 7.3. All chemicals, unless otherwise stated, were obtained from Sigma.

Signals were processed using an EPC-7 amplifier (Heka Elektronik, Lambrecht, Germany). Series resistance was <20 MΩ for nystatin perforated patch-clamp recordings and compensated at 70–80%. An Ag–AgCl electrode connected to the bath solution via a KCl–agar bridge served as reference. All signals were digitized at 5 kHz, filtered at 2 kHz, and stored on computer for off-line analysis. Data were collected using pClamp 6.0 software (Molecular Devices). The membrane potential was held at −70 mV and stepped to levels between −120 and +120 mV in 20 mV increments.

Immunohistochemistry. Adult rats were anesthetized with sodium pentobarbital (60 mg/kg, i.p.) and perfused through the left ventricle with a PBS solution (100 mM Na_2HPO_4/NaH_2PO_4, pH 7.4, and 150 mM NaCl) containing 0.5% $NaNO_2$ and 1000 U heparin, followed by a phosphate buffer (PB) solution (100 mM Na_2HPO_4/NaH_2PO_4, pH 7.2) containing 4% paraformaldehyde. Brains were removed, postfixed in 4% paraformaldehyde for 2 h at 4°C, rinsed twice with PB, and then placed either in 30% sucrose at 4°C for 24 h or immediately sliced sagittally on a vibratome at 20 μm. Brains not sectioned were embedded in O.C.T. compound (Tissue-Tek, Torrance, CA), rapidly frozen in acetone containing dry ice, and stored at −80°C until cryostat sectioning. Sagittal (20 μm) slices were collected in multiwell plates containing PBS. Slices were then postfixed in 4% paraformaldehyde for 5 min, followed by two washes with PBS (for 5–10 min on orbital shaker). Slices were then permeabilized with a PBS solution containing 1% bovine serum albumin (BSA), 5% normal donkey serum, 0.2% glycine, 0.2% lysine, and 0.2% Triton X-100 (blocking solution) for 1 h at room temperature or 4°C overnight and were rinsed twice with PBS containing 1% BSA alone. At this point, slices were processed for immunofluorescence.

Free-floating sections were processed for double labeling with either chicken anti-Slack (800 ng/ml) or chicken anti-Slick (1.5 μg/ml) and rabbit anti-mGluR1α (1;200; catalog #AB 1595; Chemicon, Temecula, CA) or rabbit anti-mAChR1(1:200; catalog #AMR-001; Alomone Labs, Jerusalem, Israel). After 48 h at 4°C incubation in primary antibody, sections were washed three times 10 min each. Slack and slick were localized with donkey anti-chicken cyanine 3 (Cy3) (Jackson ImmunoResearch, West Grove, PA) for 30 min at room temperature. Alexa Fluor donkey anti-rabbit 488 (Invitrogen) was used to identify mGluR1, and Alexa Fluor donkey anti-goat 488 was used to identify mAChR1. Sections were mounted on gelatin-coated slides, air dried, and coverslipped with 2.5% DL-2-amino-5-phosphonovaleric acid/1,4-diazabicyclo(2.2.2) octane (PVA-DABCO). The antibodies for both Slick (Slo2.1) and Slack (Slo2.2) were used in previous studies in which additional controls are

reported (Bhattacharjee et al., 2002, 2003). Control sections were processed through similar immunohistological procedures, except that primary or secondary antibodies were omitted. In all cases, the omission of primary or secondary antibodies resulted in the lack of specific labeling, confirming the specificity of immunocytochemical analysis.

Primary cell cultures. Primary hippocampal cultures were prepared from embryonic day 18–19 rat brains as described previously (Brewer et al., 1993) and grown in Neurobasal medium supplemented with B27 (Invitrogen). Neurons were plated on coverslips coated with poly-D-lysine (30 μg/ml) and laminin (2 μg/ml) at a density of 50,000 per well. At 14 d *in vitro* (i.e.) cells were washed twice with 1× PBS with 1% BSA, fixed in 4% paraformaldehyde in PB, pH 7.4, for 20 min, and then blocked with blocking solution for 1 h at room temperature or at 4°C overnight. After adding the primary antibodies against Slick or Slack with those against mGluR1 or mAChR1, cultures were agitated either for 1 h at room temperature or at 4°C overnight. Cultures were then washed three times 10 min each, and fluorescent labeled secondary antibodies were added for 30 min (chicken Cy3 at 1:400 for Slack and Slick; Alexa Fluor 488 donkey anti-rabbit at 1:400 for mGluR1 and mAChR1). Cover glasses were then washed with 1× PBS with 1% BSA three times 10 min each and then mounted on glass slides with anti fading 2.5% PVA-DABCO solution. Images were taken immediately with a Zeiss (Oberkochen, Germany) laser scanning microscope (LSM 510, LSM META, or LSM NLO). DAB staining was performed on hippocampal cultures to confirm the staining patterns. A variety of controls were performed to determine whether there was any cross-reactivity between antibodies: (1) chicken anti-Slick or -Slack primary antibodies were used with donkey anti-rabbit Cy3 secondary antibodies; (2) chicken anti-Slick or -Slack primary antibodies were used with donkey anti-goat Cy3 secondary antibodies; (3) primary antibodies were omitted and donkey anti-chicken Cy3 secondary antibodies were used with either Alexa Fluor 488 donkey anti-rabbit or with Alexa Fluor 488 donkey anti-goat antibodies. No staining was observed in any of these conditions.

Image acquisition and analysis. Sections were examined with a Zeiss laser scanning microscope (LSM 510, LSM META, or LSM NLO) coupled to a computer with Zeiss image acquisition and analysis software. Images were acquired in the multi-track mode, because this function permits several tracks to be defined as one configuration for the scan procedure and this does not allow fluorescence to bleed into the other channel. Images were acquired using C-Apochromat 40×/1.2 or 63× objective (water correction) for brain slices as well as for hippocampal cultures, and the optical thickness of the slices was constant for both tracks. Alexa Fluor 488 has excitation/emission of 496/519, and Cy3 has antibodies/emission of 550/570. Double-immunofluorescence images were also displayed as dual-color merged images. We used Adobe Photoshop (Adobe Systems, San Jose, CA) to sharpen images, adjust brightness and contrast level, and compose final plates. The scale bar on hippocampal images and brain sections represents 20 μm.

Results

Slo2.1 and Slo2.2 channels have similar primary sequences

Four high-conductance potassium channels of the Slo family are encoded in the mammalian genomes. All four genes are located on different chromosomes, suggesting an ancient origin in evolution. These channels share a common feature with the extended gene family of voltage-dependent potassium channels in having six homologous membrane-spanning domains per α subunit (S1 through S6), which surround the permeation pathway of the channel. (Note that Slo1 and Slo3 have an additional membrane-spanning domain, S0, as described below.) However, Slo family channels differ in having a much larger carboxyl extension, which is thought to be entirely cytoplasmic and involved with modulation of channel function by cytoplasmic factors (Schreiber and Salkoff, 1997; Vergara et al., 1998; Moss and Magleby, 2001; Bao et al., 2002; Shi et al., 2002; Tang et al., 2004; Zeng et al., 2005). All four of the encoded peptides are similar in length. The four known genes fall into two subgroups defined by the closely related paralogs, Slo2.1/Slo2.2 and Slo1/Slo3. These two groupings are evident in the hydrophobicity plots shown in Figure 1 in which Slo2.1/Slo2.2 clearly show greater similarity than Slo1/Slo3.

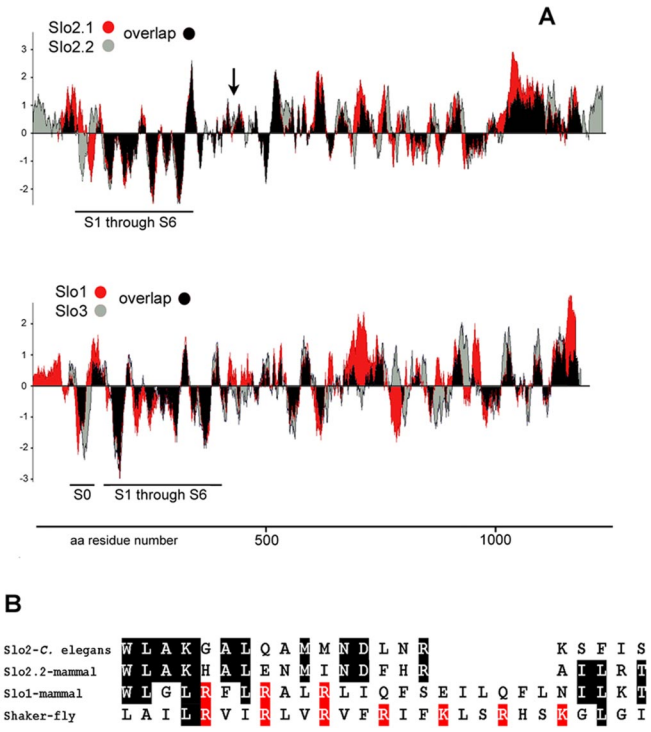

Figure 1. ***A***, Hydrophobicity plot of Slo family channels showing that the four Slo family channels fit into two distinct subgroups. Slo2.1 and Slo2.2 lack the extra membrane spanning segment (S0) found in Slo1/Slo3. In both grouped pairs, the highest similarity (black shading) is in the S1–S6 membrane-spanning domains and in the immediately adjacent downstream region. Hydrophobicity analysis used the Kyte–Doolittle program (Kyte and Doolittle, 1982). Arrow indicates site of exchange in the construction of the C1 chimera (see Results). ***B***, Alignment of residues in the S4 regions of the Slo2 channel from *C. elegans*, Slo2.2 (Slack) from humans and rodents, Slo1 from humans and rodents, and the voltage-sensitive Shaker channel from *Drosophila.* A string of positively charged amino acids occurring every three residues is found in the S4 region of voltage-dependent channels. Such charges at the appropriate interval are shaded in red and indicated in the voltage (and calcium) dependent Slo1 channel and in the voltage-dependent Shaker (Kv1) channel. Such a string of positive charges at the appropriate intervals is absent in Slo2 channels, and the overall region is six residues shorter than in voltage-dependent channels.

Two main structural features distinguish Slo2.1/Slo2.2 from Slo1/Slo3. Slo2.1/Slo2.2 channels lack the typical arrangement of positively charged residues in S4 associated with voltage-dependent gating, which is found in all voltage-gated potassium channels, including Slo1/Slo3 (Fig. 1*B*). Indeed, the S4 region in Slo2 channels appears to have six fewer residues overall compared with S4 in voltage-sensitive channels and, thus, may have a radically different orientation in the channel protein. Also, Slo2.1/Slo2.2 lack the extra membrane spanning domain (S0) near the N-terminal of Slo1/Slo3 that results in placing the N-terminal outside of the cell (Meera et al., 1997; Schreiber et al., 1998). Slo2.1/Slo2.2 paralogs have high amino acid sequence similarity (74% identity in humans, which contrasts with the lower Slo1 and Slo3 identity of ~43%), with highest similarity in the membrane-spanning domains (Fig. 1). Slo2.1/Slo2.2 have highly conserved mammalian orthologs. Rat and human Slo2.1 channels have >95% identity, and rat and human Slo2.2 channels have >91% identity (Bhattacharjee et al., 2003; Yuan et al., 2003). Interestingly, the main sequence divergence between

Slo2.1/Slo2.2 channels resides in the C terminus (Fig. 1), which we will show to be important for their modulation by PKC.

Slo 2.1 and Slo2.2 share basic functional properties

Expression of Slo2.1 and Slo2.2 channels was tested in *Xenopus* oocytes using two-electrode voltage clamp, 3–5 d after cRNA injection (Fig. 2). Both channels produced noninactivating outward K^+ currents, with tails reversing at approximately −70 mV. Currents were blocked by extracellular tetraethylammonium in a concentration range between 70 and 150 mM. Typically, Slo2.1 current amplitudes were smaller than those of Slo2.2 (Fig. 2*A*). Slo2.1 channels were also more difficult to express than Slo2.2 channels, being observed in only 25% of injected oocytes, thus making single-channel recordings difficult to obtain. Consistent with a previous report (Bhattacharjee et al., 2003), Slo2.1 currents showed faster kinetics of activation than those of Slo2.2 (Fig. 2*A*). Also consistent with previous reports (Bhattacharjee et al., 2003; Yuan et al., 2003), both channels showed Na dependence and were activated by the application of 80 mM Na^+ to the intracellular surface of inside-out patches. The Na dependence for the human clone of Slo2.1 was similar to that reported for rat Slo2.1 expressed in CHO cells (Fig. 2*B*) (Bhattacharjee et al., 2003) and similar to that reported for Slo2.2 (Yuan et al., 2003). However, the mean single-channel conductance for hSlo2.1 was 60 pS, which was smaller than the 140 pS described for rSlo2.1. This discrepancy might be partially explained by the fact that we used 80 mM symmetrical K^+, instead of 130 mM used previously (Bhattacharjee et al., 2003). Both currents showed very weak voltage dependence, reflected in the slope values obtained from fitted *I–V* curves in Figure 2*C*, a fact consistent with the lack of a conventional S4 voltage-sensing region (Fig. 1*B*). Low voltage sensitivity is also evident in ramps obtained from cell-attached patches. Single-channel openings can be clearly distinguished at potentials even more negative than the resting potentials of many cells (Fig. 2*D*). Control recordings in uninjected oocytes did not show any currents with the characteristics described above. The low sensitivity to voltage permits Slo2 channels to affect the resting potential of a cell, potentially controlling basal electrical excitability.

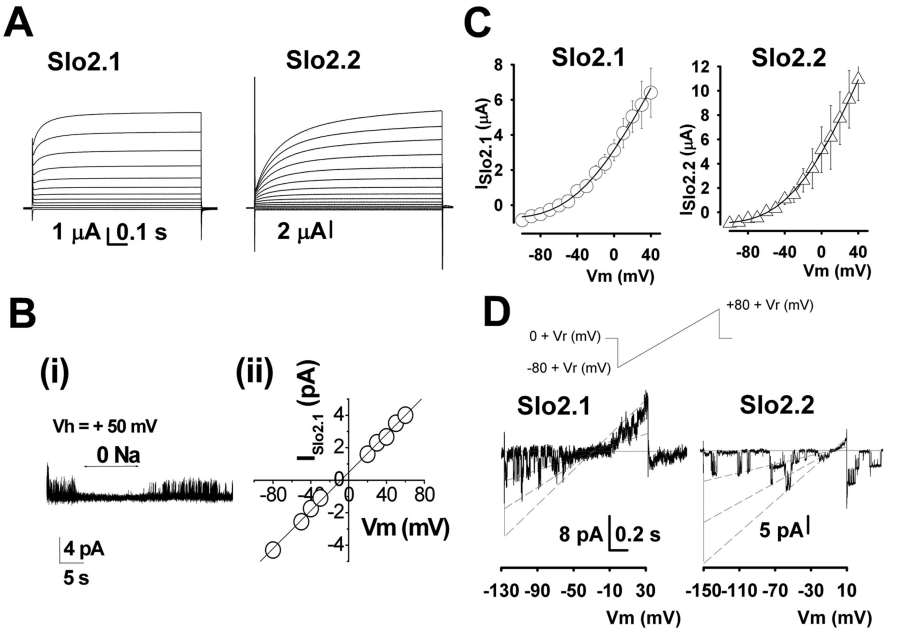

Figure 2. Functional properties of Slo2 channels expressed in *Xenopus* oocytes. ***A***, Whole-cell currents of Slo2 channels. Records were obtained with two-microelectrode voltage clamp. V_h was −80 mV, in 10 mV voltage steps. ***B***, Human Slo2.1 cRNA expresses a high-conductance Na-sensitive K^+ channel. ***Bi***, Single-channel Slo2.1 currents from an inside-out patch held at +50 mV and perfused with 80 mM Na or 0 Na, as indicated. Symmetric (80 mM) K^+ was used in this experiment. ***Bii***, Mean current–voltage relationship of single channels from multiple patches ($n = 5$). The single-channel conductance in 80 mM symmetrical K^+ is 59 ± 0.001 pS (mean ± SE). ***C***, Slo2 channels have shallow voltage dependence. Average current–voltage relationship for whole-cell Slo2 currents at V_h of −60 mV ($n = 23$ for Slo2.1 and $n = 13$ for Slo2.2). Open circles represent Slo2.1, and open triangles represent Slo2.2. Solid lines are the best fit of $I = g \times (V_m - V_k)$, where $g = g_{max}/(1 + \exp(-(V_m - V_{1/2}/K)))$. Parameters for the best fit were as follows: for Slo2.1, $V_{1/2} = -23 \pm 9$ mV, $K = 51 \pm 5$ mV, $g_{max} = 0.087 \pm 0.002$ mS; for Slo2.2, $V_{1/2} = -15 \pm 8$ mV, $K = 48 \pm 6$ mV, $g_{max} = 0.14 \pm 0.02$ mS. Note that the slope factor K is quite high, indicating low intrinsic voltage sensitivity. ***D***, Slo2 channels are active at negative potentials near the resting potential. Records elicited by ramps at indicated voltages are shown. Because records were obtained in the cell-attached configuration, the resting potential (V_r of approximately −80 mV) had to be taken into account to estimate the true membrane potential. [K^+] in the pipette was 80 mM. Note that both channels are active at potentials even more negative than the usual cell resting potentials.

Slo2.1 and Slo2.2 channels are oppositely modulated by PMA

Because Slo2.1 and Slo2.2 have only slight voltage sensitivity, we considered the possibility that these channels might be modulated by factors in addition to Na^+ and Cl^-, possibly involving second-messenger systems. In considering this possibility, we noticed that several putative PKC phosphorylation sites were identified previously that are unique to one or the other channel (Bhattacharjee et al., 2003). Hence, we investigated whether Slo2.1 and Slo2.2 channels were subject to PKC modulation. Both Slo2 channels were expressed in *Xenopus* oocytes and exposed to the specific and potent PKC activator PMA. Figure 3 shows that the application of very low (nanomolar) concentrations of PMA had profound and opposite effects on the amplitude of Slo 2.1 and Slo2.2 whole-cell currents. Slo2.1 whole-cell currents were reduced by ~90% after addition of 60 nM PMA to the bath solution. In contrast, Slo2.2 whole-cell currents were substantially increased after application of PMA (Fig. 3*A*). The inhibition of Slo2.1 currents occurred at all voltages (Fig. 3*B*). Notably, oocyte resting potentials were depolarized by ~20 mV after application of PMA (from approximately −50 to −30 mV), suggesting that the Slo2.1 current contributed to the cells resting conductance. In contrast, Slo2.2 currents were increased approximately fivefold by 160 nM PMA, and the application of PMA to Slo2.2-expressing oocytes caused an increase in the cell resting potential of approximately −15 mV. Slo2.1 currents were inhibited by PMA with an IC_{50} of ~20 nM, whereas the increase in Slo2.2 currents had an IC_{50} of ~50 nM (Fig. 3*C*). The inhibition of Slo2.1 currents at a concentration of 20 nM PMA reached a maximal effect in 6–10 min (time constant, ~2 min; voltage test pulse at +20 mV) (Fig. 3*D*). Stimulation of Slo2.2 took ~4 min to half-saturation. The time course for PMA action observed here is consistent with reports in the literature for the effects of PKC on several membrane proteins and channels (Covarrubias et al., 1994; Boland and Jackson, 1999). The experiments described above were undertaken in the *Xenopus* oocyte expression system, but similar results were seen when HEK-293 cells were used as the heterolo-

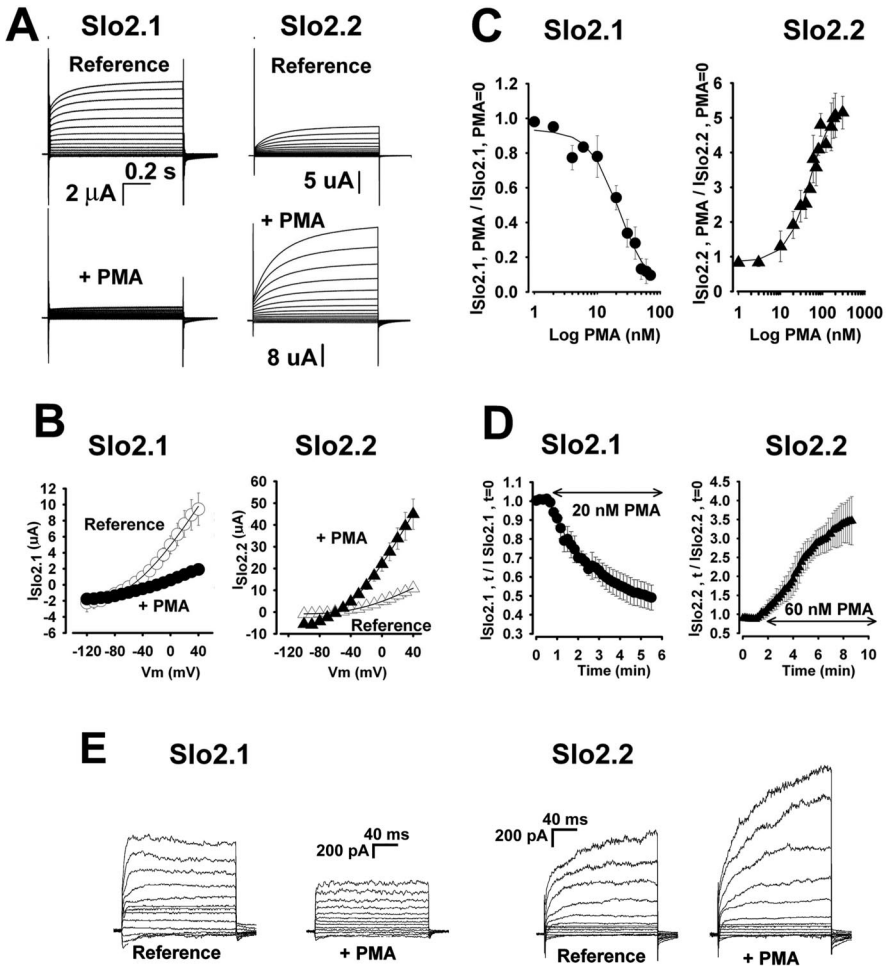

Figure 3. Phorbol ester has opposite effects on Slo2.1 and Slo2.2 channels expressed in *Xenopus* oocytes and HEK cells. ***A***, Effect of PMA on whole-cell records of Slo2.1 and Slo2.2. Top traces, Currents recorded before the addition of PMA; bottom traces, currents recorded after the addition of 60 nM PMA for Slo2.1 and 160 nM PMA for Slo2.2. ***B***, PMA oppositely affects Slo2 currents at all voltages. Open symbols, Average current–voltage relationship before PMA exposure. Filled symbols, Current–voltage relationship after treatment with 60 nM PMA for Slo2.1 ($n = 9$) and 160 nM PMA for Slo2.2 ($n = 10$). ***C***, Dose–response curves for PMA. Current is plotted as a function of PMA concentration. Note the semilog scale for Slo2.1 (left) and Slo2.2 (right). Test pulses were at 20 mV. Solid lines show the best fit (sigmoidal) of dose–response curves. IC_{50} was 20 nM for Slo2.1 and 50 nM for Slo2.2. The Hill coefficient was similar in both cases (1.6). Although both channels are sensitive to PMA, Slo2.1 is more sensitive than Slo2.2. ***D***, Response of Slo2 channels to PMA develops in minutes. Left, Onset of inhibition for Slo2.1 exposed to 20 nM PMA; right, onset of current enhancement for Slo2.2 exposed to 60 nM PMA. Test pulses were at 20 mV. ***E***, PMA decreases the amplitude of Slick (Slo 2.1) currents and increases the amplitude of Slack (Slo 2.2) currents in HEK-293 cells. In nystatin perforated patch-clamp recordings, whole-cell K^+ conductances were evoked by voltage steps between −120 and +120 mV in 20 mV increments from a holding potential of −70 mV. Bath application of PMA (100 nM) produced a rapid decrease in Slo2.1 and increase in Slo2.2 currents (currents started to change in 3–5 min after PMA application).

gous system. In nystatin perforated patch-clamp recordings, bath application of PMA (100 nM) produced a rapid decrease in Slick whole-cell K^+ currents and an increase in Slack currents (Fig. 3*E*).

In *Xenopus* oocytes, the PMA effects on Slo2.1 and Slo2.2 were not reversed after 10 min of wash, suggesting a long-lasting effect of phosphorylation by PKC. PMA effects on both channels were almost completely eliminated by preincubation (8–12 h) in 1 μM staurosporin, a kinase blocker highly effective for PKC ($n = 15$). Also, modulatory effects were not seen in control experiments using 4-αPMA, an inactive analog of PMA, in concentrations up to 200 nM ($n = 2$). Additional evidence implicating PKC was achieved by experiments using the membrane permeant analog of diacylglycerol (DAG), 1-oleoyl-2-acetyl-*sn*-glycerol (OAG). Results of these experiments adding 30–40 μM OAG to the bath instead of PMA produced essentially the same results as PMA (data not shown). Because DAG is a second-messenger activator of PKC, this is additional evidence of the involvement of PKC. We thus conclude that the activation of PKC had opposite modulatory effects on Slo2 channels, activating Slo2.2 and inhibiting Slo2.1. Considering that Slo2.1 and Slo2.2 are high-conductance channels, even a minor fraction of these channels open at normal cell resting potentials of cells might permit PKC regulation of action potential threshold and basal cell excitability. The differential modulation by PKC of these two channels would thus have opposite functional implications; inhibition of Slo2.1 would increase excitability, whereas the stimulation of Slo2.2 would decrease it.

Transfer of inhibition by PMA to Slo2.2 by swapping Slo channel tails

Modulation of potassium channels by intracellular factors often occurs through the interaction of such factors with structural domains on the carboxyl oriented "tail" of the channel. The tail of the channel describes the cytoplasmic region that follows the membrane-spanning domains of the pore-forming "core" of the channel (Wei et al., 1994; Meera et al., 1997; Quirk and Reinhart, 2001). We noticed that several putative PKC phosphorylation sites were identified previously as unique to Slo2.1 and present on the tail of the channel. If the PMA-induced inhibition of Slo2.1 involved this region, a revealing demonstration to support this would be to construct a chimera, transplanting the tail of Slo2.1 onto the core of Slo2.2. If the hypothesis were correct, the action of PMA should inhibit rather than enhance the currents produced by this chimera. We therefore constructed the chimera (C1) that had the core of Slo2.2 and the tail of Slo2.1 ligated in-frame at a junction point immediately after the core (Figs. 1, 4*A*, arrows). The C1 construct expressed large currents similar to currents from Slo2.2 channels, albeit with faster activation kinetics (Fig. 4*B*). Like Slo2.2, C1 displayed shallow voltage dependence, sensitivity of gating to intracellular Na, and high unitary conductance (Fig. 4*B*,*C*). However, the effect of PMA on C1 was strikingly similar to that of Slo2.1 and unlike that of Slo2.2 (Fig. 5). Application of 20–50 nM PMA to oocytes expressing C1 currents caused significant inhibition (Fig. 5*A*). Application of 20 nM PMA reduced the C1 current ~75% (Fig. 5*B*). Similar results were obtained from cell-attached patches (Fig. 5*C*). The cell-attached patch recordings shown in Figure 5*C* show a patch with three channels at −40 mV. After addition of 40 nM PMA, the activity diminished dramatically. The diminished current was mainly the result of lowered open-state probability (NPo); single-channel conductance was unaffected. When currents were evoked by linear ramps from −80 to +80 mV, PMA reduced C1 single-channel openings at all

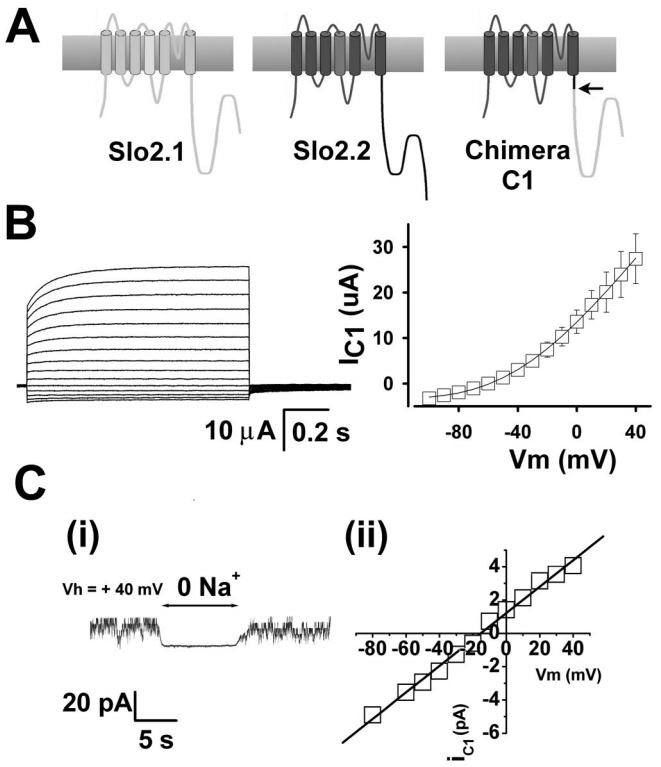

Figure 4. Slo2.2/Slo2.1 chimeric channels express well and retain basic properties. ***A***, Chimera (C1). C1 was constructed with the Slo2.2 core and the Slo2.1 tail. Site of ligation is indicated by arrow (see Materials and Methods). ***B***, C1 has weak voltage dependence. Currents elicited by 10 mV step pulses from a holding potential of −60 mV are shown to the left. Average current–voltage relationship is shown on the right ($n = 9$). Best-fit parameters were similar to those of Slo2.1 and Slo2.2. Current expression levels were usually much higher than those of Slo2.1 or Slo2.2 channels. ***C***, C1 chimera is a high-conductance Na-activated K^+ channel. ***Ci***, Currents from an inside-out patch expressing C1 channels. Single-channel currents were continuously recorded at +40 mV in the presence or absence of 80 mM intracellular Na. ***Cii***, Mean *I–V* relationship from $n = 14$ patches. The unitary conductance was 79 ± 0.002 pS (mean ± SE), similar to Slo2.2 (88 pS).

voltages. Similar results were obtained in several cell-attached patches, consistent with experiments using the two-microelectrode technique. Cell-attached experiments done as a control with Slo2.2 showed an opposite result; currents greatly increased after 1 min of PMA application (Fig. 5*D*). As with Slo2.1 and Slo2.2, incubation of the C1-injected oocytes in staurosporine prevented the action of PMA ($n = 6$). The inactive PMA analog 4-αPMA, had no modulatory effect on C1 currents ($n = 2$). Thus, all results support the conclusion that the PMA sensitivity by Slo2.1 is mediated by its C-terminal tail. The converse chimera (Slick core and Slack tail) was synthesized but had very low and inconsistent expression, and we were unable to determine whether PMA affected the level of current. However, we constructed a second chimera whose functional properties further supported the general hypothesis that the cytoplasmic tail altered modulation by PMA. This construct had the core of Slack (Slo2.2) with the tail of Slo1 ligated at the same restriction site used to construct the C1 chimera. This construct expressed large currents (Fig. 5*E*). However, these currents showed no response to PMA, neither increasing nor decreasing after PMA application (Fig. 5*E*). Thus, to summarize, the Slo2.1 channel is negatively regulated by PMA, the Slo2.2 channel is positively regulated by PMA, the chimera having the core of Slo2.2 and tail of Slo2.1 is negatively regulated by PMA, and, finally, the chimera having the core of Slo2.2 and tail of Slo1 is insensitive to PMA. Together, these results support the hypothesis that domains in the tail markedly influence the modulatory response of the channel to PMA and that negative regulation by PMA is likely to be attributable to domains in the Slo2.1 tail.

To determine whether PKC phosphorylation plays a major role in C1 inhibition and consequently in Slo2.1 inhibition, we took advantage of the high levels of single-channel expression of C1 and compared the effect of PMA with that of PKC directly applied to the intracellular surface of the channel. Figure 6*Ai–Aiii* illustrates an experiment in which we applied PKM (a constitutively active form of PKC) (Pontremoli et al., 1990) to the cytoplasmic face of the channel in inside-out patches. First, we demonstrated single-channel activity from C1 in a cell-attached patch, with ramps from −80 to +80 mV. Two channels are clearly seen in the patch (*Ai*). The patch was then excised to a bath solution with low concentrations of Na^+ and Cl^- (20 and 40 mM, respectively), similar to those present in the egg cytoplasm (Cooper and Fong, 2003) (*Aii*). Under these conditions, the two channels remained active at a level comparable with that seen in the cell-attached configuration. Finally, the intracellular side of the patch was perfused with 0.1 U/ml PKM (containing 200 μM ATP-Mg). After treatment and return to the bath solution, channel activity in the patch diminished dramatically (*Aiii*). This result could be seen clearly in a continuous recording obtained from a test voltage of +40 mV (Fig. 6*B*). After 1–2 min of perfusion with PKM, the activity of the channel decreased by six times (NPo diminished from 0.6 to 0.1). Inhibition of single-channel activity by PKM was also seen in three other patches. In such experiments, channel rundown is a potential factor to be considered. However, we noted that rundown, when it occurred, usually developed very fast (<1 min). Thus, we took care to use membrane patches that had stable recording properties for several minutes, with no apparent rundown. Control experiments with direct application of PMA to the intracellular surface of excised patches did not show any effect.

Direct action of PMA-stimulated PKC on the channel may produce a long-lasting effect. Presumably, after PMA treatment of an oocyte, C1 channels would be phosphorylated and remain inhibited, even after patch excision. To test this hypothesis, single-channel activity was first recorded in the cell-attached patch configuration. The oocyte was then exposed to 40 nM PMA. After 1–2 min of exposure, channel activity was almost completely inhibited (Fig. 6*C*). This low state of activity remained significantly lower than in the pretreated cell-attached condition and persisted for at least 5 min. After excision of the patch, the low level of activity persisted at a similar level (Fig. 6*Ciii*). These experiments suggest that, at least in part, the inhibitory effect of PKC may be attributable to a direct phosphorylation of the Slo2.1 tail. However, we cannot rule out the possibility that there is an accessory protein associated with the channel that is the target of PKC-stimulated phosphorylation.

Slo2.1 and Slo2.2 channels are modulated by neurotransmitters

Activation of PKC is an integral part of the signaling cascade elicited by neurotransmitter stimulation of $G\alpha_q$-coupled protein receptors. We noted that Slo2 channels are expressed in many regions of the brain in which $G\alpha_q$-coupled protein receptors are present (Pontremoli et al., 1990; Hoffman and Johnston, 1998; Marinissen and Gutkind, 2001; Brady and Limbird, 2002; Cooper and Fong, 2003; Kroeze et al., 2003; Breitwieser, 2004; Rashid et al., 2004). Examples include hippocampal neurons of the CA1

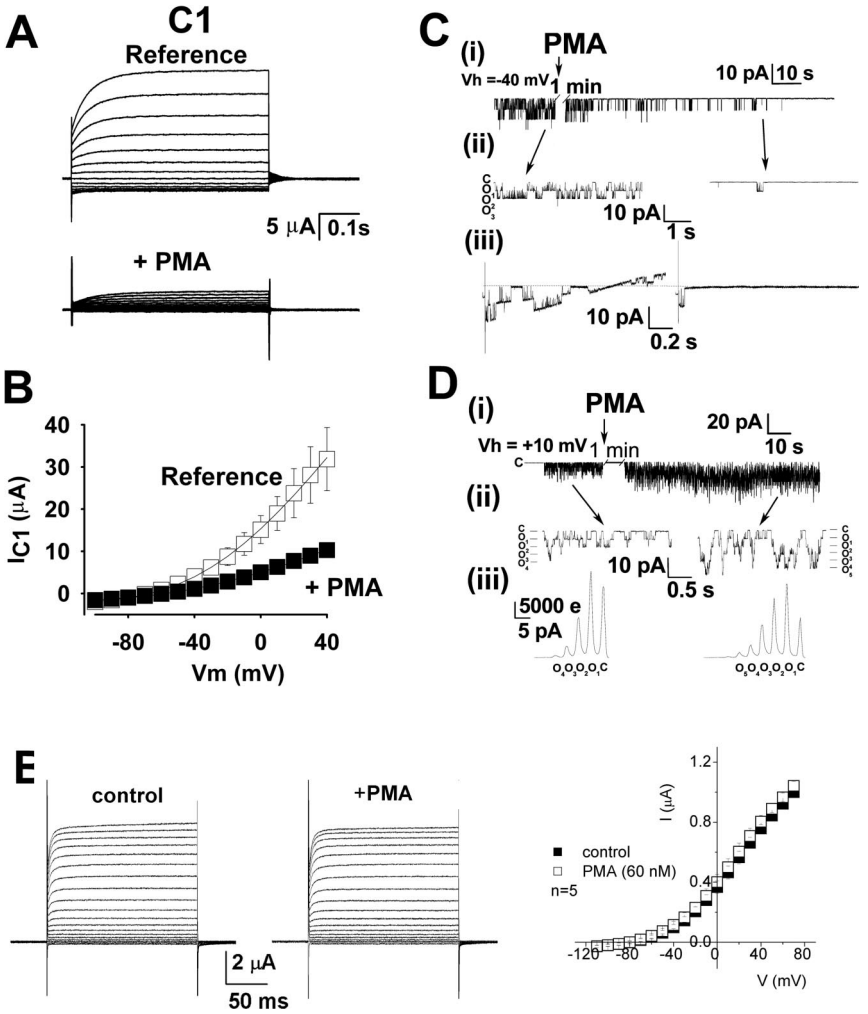

Figure 5. PMA inhibits C1 currents but stimulates Slo2.2. ***A***, C1 whole-cell currents before and after addition of 20 nM PMA. ***B***, Average current–voltage relationship before and after addition of 20 nM PMA ($n = 8$). ***C***, Inhibition of C1 single channels by PMA. Continuous recordings from cell-attached patches were obtained at −40 mV before and after the application of 40 nM PMA. Records are shown at compressed (***i***) and expanded (***ii***) time scales. Before exposure to PMA, three active channels can be seen in the patch indicated as O_1–O_3. PMA caused inhibition in ~2 min. NPo (measured for 10 s intervals) decreased from 1.2 to 0.028. ***Ciii***, Single-channel recordings obtained with ramps from −80 to +80 mV from a holding potential of 0 mV before (left) and after (right) 40 nM PMA. ***D***, Slo 2.2 single-channel activity is increased by PMA. Cell-attached recordings at +10 mV are shown at compressed (***i***) and expanded (***ii***) time scales. After applying 40 nM PMA for 2 min, additional Slo2.2 channels are active. Before the application of PMA, four levels of unitary conductance can be seen (O_1–O_4) and NPo was 1.1. After treatment with PMA, five levels of unitary conductance were observed (O_1–O_5) and NPo increased to 3.8. The recruitment of Slo 2.2 channels by PMA is also illustrated with histograms obtained for 40 s intervals (***iii***). ***E***, Control experiments with Slo1 tail grafted to the Slack core show no effect of added PMA. Current traces show the Slack/Slo1 chimera currents in control conditions and in the presence of 60 nM PMA as labeled. Currents were elicited from a V_h of −90 mV, with test pulses ranging from −110 to +70 mV in 10 mV steps. The effect of PMA (60 nM) was measured after 6 min of the application of the drug. The graph at the right shows the mean normalized current–voltage relationships of the Slack/Slo1 chimera in control conditions (filled squares) and in the presence of 60 nM PMA (open squares) for five oocytes in each condition.

region, in which Slo2.1 channels are abundant (Bhattacharjee et al., 2003). Conceivably, in some cells, Slo2 channels and $G\alpha_q$-coupled receptors may be coexpressed and functionally coupled (Fisahn et al., 2002). To test whether such functional coupling was possible, we coexpressed $G\alpha_q$ receptors and Slo2 channels in the *Xenopus* oocyte expression system. Examples of such experiments are shown in Figure 7, in which we reconstituted the functional coupling between both Slo2 channels and the M_1 receptor. As might be expected from the results obtained with PMA, stimulation of the M_1 receptors by 5–40 μM oxotremorine (a specific agonist of the M_1 receptor) inhibited Slo2.1 currents, whereas it augmented Slo2.2 (Fig. 7*A*). The average current–voltage relationships are shown in Figure 7*B*. Similar experiments were also performed with AT1B and mGluR1. In each case, the results were consistent with those obtained with the M_1 receptor (data not shown). (Angiotensin II was used to stimulate the AT1B receptors, whereas mGluR1 receptors were stimulated by the agonist 1-aminocyclopentane-1,3-dicarboxylic acid.) Receptors of these types are known to be expressed in hippocampus, in which they are likely to modulate neuronal excitability (Mannaioni et al., 2001; Ireland and Abraham, 2002). In control experiments, application of the above agonists to oocytes injected only with Slo2 channels did not have any effect. Also, the expression of the receptor alone either with or without the agonists did not produce currents larger than endogenous background currents.

Slo2 channels and $G\alpha_q$-coupled protein receptors are coexpressed in the CNS

To gain additional evidence for the hypothesis that Slo2 channels are regulated through activation of the M_1 and mGluR1α receptors *in vivo*, as well as in our reconstituted system, we undertook coimmunostaining experiments on rat brain sections, as well as on primary cell cultures of neurons derived from the hippocampus. The goal of these colabeling experiments was to verify that both receptors and channels could be expressed in the same types of identified cells. Both Slo2.1 and Slo2.2 are very widely expressed throughout the CNS (Bhattacharjee et al., 2002, 2005). Figure 8 shows some examples of colocalization. For example, Slo2.1 is expressed in neurons of the prefrontal cortex, in which mAChR1 receptors are also strongly expressed (Levey et al., 1991). Clear colocalization of receptors and Slo2.1 channels can be observed (Fig. 8*A*). The Slo2.2 channel is less widely expressed in cortex but is found in certain neurons of frontal cortex (Bhattacharjee et al., 2002). Figure 8*B* shows colocalization of Slack (Slo2.2) with mAChR1 in a subset of neurons of layer V of frontal cortex. In hippocampus, the Slick (Slo2.1) channel is expressed in both CA1 and CA3 regions, in which it colocalizes with the mAChR1 receptor (Fig. 8*C*,*D*) (Levey et al., 1995; Bhattacharjee et al., 2005). Finally, mGluR1 receptors are expressed in hippocampus (Shigemoto et al., 1997). Figure 8*E* demonstrates coimmunolabeling of Slo2.1 with mGluR1α in cultures of hippocampal neurons. The observed pattern of staining is consistent with colocalization of Slo2.1 and mGluR1 at the plasma membrane. In general, in this and previous studies, Slo2.1 and Slo2.2 channels appear to be most prominently localized in the soma and initial segments in which they conceivably could play an important role in the integrative properties of neurons.

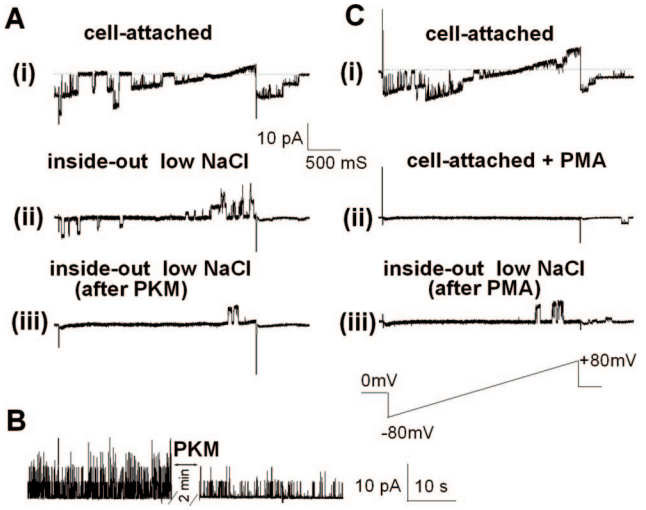

Figure 6. Comparison of the effects of PMA and PKM on C1 channels. ***A***, The activity of C1 chimeric channels in inside-out patches is reduced by PKM. Records were obtained with the ramp protocol shown at the bottom of the figure. ***Ai***, Cell-attached patches. ***Aii***, Cell-attached patches excised in low NaCl solution. ***Aiii***, Reduced single-channel activity after perfusion of the cytoplasmic surface with 0.1 U/ml PKM. ***B***, Reduction of single-channel activity after PKM application seen in continuous recordings from inside-out patches held at +40 mV. Effects of PKM were clearly seen after 2 min of perfusion of 0.1 U/ml PKM. NPo values are 0.6 before and 0.1 after 2 min of application of PKM. ***C***, Reduced activity of C1 channels from oocytes treated with PMA persists in excised patches. Records were obtained with the ramp protocol shown in the figure. ***Ci***, Single-channel activity in cell-attached patches. ***Cii***, Oocytes were treated with 40 nM PMA, and inhibition of channels in cell-attached patches was observed. ***Ciii***, Single-channel activity observed in excised patches of PMA-treated oocytes remains low, indicating that PMA promotes a long-lasting modification of the channel, independent of possible cytosolic factors.

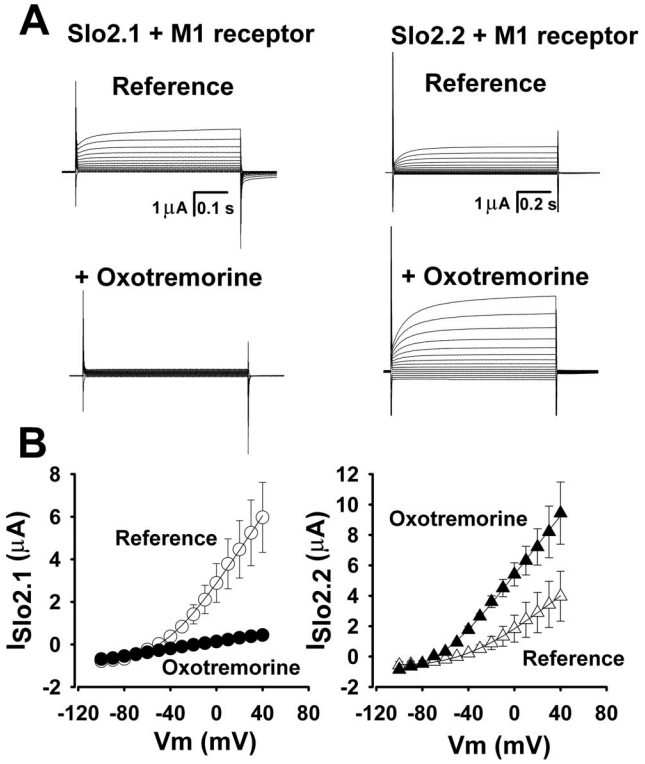

Figure 7. Opposite modulation of Slo2.1 and Slo2.2 channels by M_1 receptor activation in *Xenopus* oocytes. ***A***, Slo2.1 and Slo2.2 currents recorded from oocytes coinjected with channel and M_1 receptor cRNA. Currents are shown before (reference) and after the addition of 30 μM oxotremorine. Slo2.1 (left) is reduced whereas Slo2.2 (right) is enhanced by oxotremorine application. Effects are attributable to stimulation of the M_1 receptors by oxotremorine because no effects by oxotremorine were observed in oocytes injected with the Slo2 channels alone (data not shown). ***B***, Average current–voltage relationship in oocytes coinjected with Slo2.1 and Slo2.2 cRNAs and the M_1 receptor. Slo2.1 currents are shown by circles ($n = 4$), and Slo2.2 currents are shown by triangles ($n = 4$). Reference conditions are shown by open symbols, and 30 μM oxotremorine is shown by filled symbols.

Discussion

Slo2 channels became known only as a result of the genomic sequencing projects, first in *Caenorhabditis elegans* and then in mammals. As a consequence of their relatively recent appearance, they are less well studied than other types of potassium channels. Slo2 channels are particularly interesting candidates with regard to their modulation by M_1 and mGluR1 receptors or potentially by other $G\alpha_q$-coupled receptors. Our results raise many interesting questions regarding the physiology of Slo2 channels. It remains to be established whether Slo2 currents account for any portion of the current activated or inhibited through muscarinic receptors *in vivo*. Conceivably, Slo2 channels could express a component of the m-current not attributable to the KCNQ family of potassium channels. Another area that now remains to be explored is the likelihood that both Slick and Slack are coexpressed in the same cells, especially in neurons that are positive for M_1, mGluR1, or other receptors linked to activation of PKC. In such cells, the two Slo2 channels may form heteromultimers. Preliminary findings from coexpression studies of the two Slo2 channels in heterologous systems indicate that Slick and Slack can indeed form heteromultimers and that, in heteromultimeric channels, the Slick subunit has a dominant effect with regard to modulation through the M_1 or mGluR1 receptor. Thus, heteromultimers are inhibited during receptor stimulation (our unpublished results). These and other questions remain to be studied in future experiments.

The high conductance of Slick and Slack and their low voltage sensitivity makes these channels ideal candidates for controlling overall cell excitability through their contribution to the resting cell conductance. The extent to which they contribute to resting cell conductance remains to be determined. However, current components that are active at rest need not be very large to have a major impact on the overall excitability of the cell. This is because total cell resting conductance is usually small and represents only a tiny fraction of the overall cell membrane conductance during peak electrical activity. A crucial factor is their contribution to the critical balance of inward and outward currents at the action potential threshold. Although both Slick and Slack require high sodium and chloride ion concentrations to be fully activated, they show substantial activity when expressed in heterologous systems in which they are exposed to physiological concentrations of these ions. Neuromodulator control of Slick and Slack currents has the potential to either decrease or increase action potential threshold. A second point regarding the effectiveness of channels in controlling overall cell excitability is their subcellular localization. Slick and Slack appear to be most concentrated in the region around and adjacent to the cell body in which incoming synaptic potentials are integrated via spatial and temporal summation. Modulation of passive membrane conductance in this region could conceivably play a crucial role in action potential generation or failure. However, although the staining colocalizes at the cellular level, much of the staining appears to be intracellular, and it remains to be determined whether the channels and receptors are indeed coexpressed on the cell surface. Thus, although the staining pattern reflects cellular coexpression, the physiological significance of this coexpression is as yet unclear and remains to

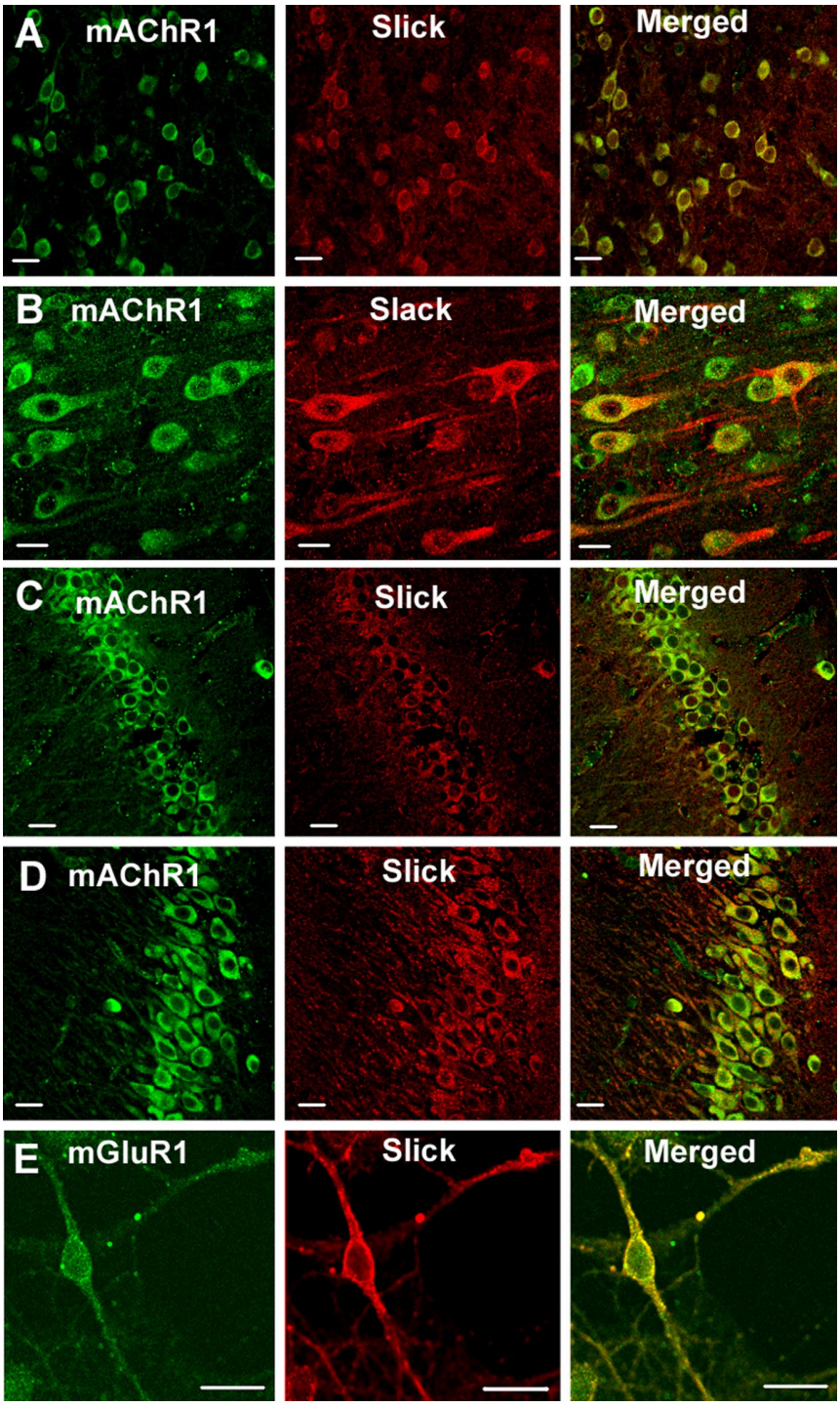

Figure 8. Colocalization of Slack and Slick with $G\alpha_q$-coupled receptors. Top 12 panels show colocalization of Slick or Slack with mAChR1 in sections of rat cortex (***A***, frontal cortex; ***B***, layer V of frontal cortex) and in hippocampus (***C***, CA1 region; ***D***, CA3 region). ***E*** shows colocalization of Slick with mGluR1α in cultures of hippocampal neurons. Slick and Slack immunoreactivity was localized with Cy3 (red), and receptor immunoreactivity was visualized using Alexa Fluor 488 secondary antibody (green). On the overlaid images, regions of colocalization appear orange to yellow. Scale bars, 20 μm.

be determined. A second possible reason for controlling resting conductance by neuromodulators in this region has to do with the dense packing of cells in the hippocampus and other brain regions. Sustained activity of densely packed mammalian central neurons is followed by a substantial transitory elevation of external K^+ concentration (Filippov and Krishtal, 1999). This phenomenon may require a mechanism whereby the resting membrane conductance can compensate for changes in the driving force of these ions. Overall, Slick and Slack through their modulation via the M_1 and mGluR1 receptors have the necessary properties to effect long-lasting changes on neuronal excitability, which could translate into major behavioral changes (Klein et al., 1982; Hochner and Kandel, 1992).

References

Adelman JP, Shen KZ, Kavanaugh MP, Warren RA, Wu YN, Lagrutta A, Bond CT, North RA (1992) Calcium-activated potassium channels expressed from cloned complementary DNAs. Neuron 9:209–216.

Atkinson NS, Robertson GA, Ganetzky B (1991) A component of calcium-activated potassium channels encoded by the *Drosophila* slo locus. Science 253:551–555.

Bao L, Rapin AM, Holmstrand E, Cox DH (2002) Elimination of the BK(Ca) channel's high-affinity Ca^{2+} sensitivity. J Gen Physiol 120:173–189.

Bhattacharjee A, Gan L, Kaczmarek LK (2002) Localization of the Slack potassium channel in the rat central nervous system. J Comp Neurol 454:241–254.

Bhattacharjee A, Joiner WJ, Wu M, Yang Y, Sigworth FJ, Kaczmarek LK (2003) Slick (Slo2.1), a rapidly-gating sodium-activated potassium channel inhibited by ATP. J Neurosci 23:11681–11691.

Bhattacharjee A, Von Hehn CAA, Mei X, and Kaczmarek LK (2005) Localization of the Na^+-activated K^+ channel slick in the rat central nervous system. J Comp Neurol 484:80–92.

Bockenhauer D, Zilberber N, Goldstein SA (2001) KCNK2: reversible conversion of a hippocampal potassium leak into a voltage-dependent channel. Nat Neurosci 4:486–491.

Boland LM, Jackson KA (1999) Protein kinase C inhibits Kv1.1 potassium channel function. Am J Physiol 277:C100–C110.

Brady AE, Limbird LE (2002) G protein-coupled receptor interacting proteins: emerging roles in localization and signal transduction. Cell Signal 14:297–309.

Breitwieser GE (2004) G protein-coupled receptor oligomerization: implications for G protein activation and cell signaling. Circ Res 94:17–27.

Brewer GJ, Torricelli JR, Evege EK, Price PJ (1993) Optimized survival of hippocampal neurons in B27-supplemented Neurobasal, a new serum-free medium combination. J Neurosci Res 35:567–576.

Brown DA, Adams PR (1980) Muscarinic suppression of a novel voltage sensitive K^+ current in a vertebrate neurone. Nature 283:673–676.

Butler A, Tsunoda S, McCobb DP, Wei A, Salkoff L (1993) mSLO, a complex mouse gene encoding "maxi" calcium-activated potassium channels. Science 261:221–224.

Chemin J, Girard C, Duprat F, Lesage F, Romey G, Lazdunski M (2003) Mechanisms underlying excitatory effects of group I metabotropic glutamate receptors via inhibition of 2P domain K^+ channels. EMBO J 22:5403–5411.

Cooper EC, Jan LY (2003) M-channels: neurological diseases, neuromodulation, and drug development. Arch Neurol 60:496–500.

Cooper GJ, Fong P (2003) Relationship between intracellular pH and chlo-

ride in *Xenopus* oocytes expressing the chloride channel CIC-0. Am J Physiol Cell Physiol 284:C331–C338.

Covarrubias M, Wei A, Salkoff L, Vyas TB (1994) Elimination of rapid potassium channel inactivation by phosphorylation of the inactivation gate. Neuron 13:1403–1412.

Dryer SE (1994) Na^+-activated K^+ channels: a new family of large-conductance ion channels. Trends Neurosci 17:155–160.

Dryer SE, Fujii JT, Martin AR (1989) A Na^+-activated K^+ current in cultured brain stem neurones from chicks. J Physiol (Lond) 410:283–296.

Filippov V, Krishtal O (1999) The mechanism gated by external potassium and sodium controls the resting conductance in hippocampal and cortical neurons. Neuroscience 92:1231–1242.

Fisahn A, Yamada M, Duttaroy A, Gan JW, Deng CX, McBain CJ, Wess J (2002) Muscarinic induction of hippocampal gamma oscillations requires coupling of the M1 receptor to two mixed cation currents. Neuron 33:615–624.

Hamill OP, Marty A, Neher E, Sakmann B, Sigworth FJ (1981) Improved patch-clamp techniques for high-resolution current recording from cells and cell-free membrane patches. Pflugers Arch 391:85–100.

Heurteaux C, Guy N, Laigle C, Blondeau N, Duprat F, Mazzuca M, Lang-Lazdunski L, Widmann C, Zanzouri M, Romey G, Lazdunski M (2004) TREK-1, a K^+ channel involved in neuroprotection and general anesthesia. EMBO J 23:2684–2695.

Hochner B, Kandel ER (1992) Modulation of a transit K^+ current in the pleural sensory neurons of *Aplysia* by serotonin and cAMP: implications for spike broadening. Proc Natl Acad Sci USA 89:11476–11480.

Hoffman DA, Johnston D (1998) Downregulation of transient K^+ channels in dendrites of hippocampal CA1 pyramidal neurons by activation of PKA and PKC. J Neurosci 18:3521–3528.

Ireland DR, Abraham WC (2002) Group I mGluRs increase excitability of hippocampal CA1 pyramidal neurons by a PLC-independent mechanism. J Neurophysiol 88:107–116.

Johnston D, Christie BR, Frick A, Gray R, Hoffman DA, Schexnayder LK, Watanabe S, Yuan LL (2003) Active dendrites, potassium channels and synaptic plasticity. Philos Trans R Soc Lond B Biol Sci 358:667–674.

Kameyama M, Kakei M, Sato R, Shibasaki T, Matsuda H, Irisawa H (1984) Intracellular Na^+ activates a K^+ channel in mammalian cardiac cells. Nature 309:354–356.

Klein M, Camardo J, Kandel ER (1982) Serotonin modulates a specific potassium current in the sensory neurons that show presynaptic facilitation in *Aplysia*. Proc Natl Acad Sci USA 79:5713–5717.

Kroeze WK, Sheffler DJ, Roth BL (2003) G-protein-coupled receptors at a glance. J Cell Sci 116:4867–4869.

Kyte J, Doolittle RF (1982) A simple method for displaying the hydropathic character of a protein. J Mol Biol 157:105–132.

Lei Q, Talley EM, Bayliss DA (2001) Receptor-mediated inhibition of G protein-coupled inwardly rectifying potassium channels involves G(alpha)q family subunits, phospholipase C, and a readily diffusible messenger. J Biol Chem 276:16720–16730.

Lesage F, Terrenoire C, Romey G, Lazdunski M (2000) Human TREK2 a 2P domain mechano-sensitive K^+ channel with multiple regulations by polyunsaturated fatty acids, lysophospholipids, and Gs, Gi, and Gq protein-coupled receptors. J Biol Chem 275:28398–28405.

Levey AI, Kitt CA, Simonds WF, Price DL, Brann MR (1991) Identification and localization of muscarinic acetylcholine receptor proteins in brain with subtype-specific antibodies. J Neurosci 11:3218–3226.

Levey AI, Edmunds SM, Koliatsos V, Wiley RG, Heilman CJ (1995) Expression of m1–m4 muscarinic acetylcholine receptor proteins in rat hippocampus and regulation by cholinergic innervation. J Neurosci 15:4077–4092.

Luk HN, Carmeliet E (1990) Na^+-activated K^+ current in cardiac cells: rectification, open probability, block and role in digitalis toxicity. Pflügers Arch 416:766–768.

Luscher C, Jan LY, Stoffel M, Malenka RC, Nicoll RA (1997) G protein-coupled inwardly rectifying K^+ channels (GIRKs) mediate postsynaptic but not presynaptic transmitter actions in hippocampal neurons. Neuron 19:687–695.

Mannaioni G, Marino MJ, Valenti O, Traynelis SF, Conn PJ (2001) Metabotropic glutamate receptors 1 and 5 differentially regulate CA1 pyramidal cell function. J Neurosci 21:5925–5934.

Mao J, Wang X, Chen F, Wang R, Rojas A, Shi Y, Piao H, Jiang C (2004) Molecular basis for the inhibition of G protein-coupled inward rectifier K^+ channels by protein kinase C. Proc Natl Acad Sci USA 101:1087–1092.

Marinissen MJ, Gutkind JS (2001) G-protein-coupled receptors and signaling networks: emerging paradigms. Trends Pharmacol Sci 22:368–376.

Meera P, Wallner M, Song M, Toro L (1997) Large conductance voltage- and calcium-dependent K^+ channel, a distinct member of voltage-dependent ion channels and seven N-terminal transmembrane segments (S0–S6), an extracellular N terminus, and an intracellular (S9–S10) C terminus. Proc Natl Acad Sci USA 94:14066–14071.

Moss BL, Magleby KL (2001) Gating and conductance properties of BK channels are modulated by the S9–S10 tail domain of the alpha subunit. A study of mSlo1 and mSlo3 wild-type and chimeric channels. J Gen Physiol 118:711–734.

Pontremoli S, Melloni E, Sparatore B, Michetti M, Salmino F, Horecker BL (1990) Isozymes of protein kinase C in human neutrophils and their modification by two endogenous proteinases. J Biol Chem 265:706–712.

Quirk JC, Reinhart PH (2001) Identification of a novel tetramerization domain in large conductance K(Ca) channels. Neuron 32:13–23.

Rashid AJ, O'Dowd BF, George SR (2004) Minireview: diversity and complexity of signaling through peptidergic G protein-coupled receptors. Endocrinology 145:2645–2652.

Schreiber M, Salkoff L (1997) A novel calcium-sensing domain in the BK channel. Biophys J 73:1355–1363.

Schreiber M, Wei A, Yuan A, Gaut J, Saito M, Salkoff L (1998) Slo3, a novel pH-sensitive K^+ channel from mammalian spermatocytes. J Biol Chem 273:3509–3516.

Shi J, Krishnamoorthy G, Yang Y, Hu L, Chaturvedi N, Harilal D, Qin J, Cui J (2002) Mechanism of magnesium activation of calcium-activated potassium channels. Nature 418:876–880.

Shigemoto R, Kinoshita A, Wada E, Nomura S, Ohishi H, Takada M, Flor PJ,. Neki A, Abe T, Nakanishi S, Mizuno N (1997) Differential presynaptic localization of metabotropic glutamate receptor subtypes in the rat hippocampus. J Neurosci 17:7503–7522.

Talley EM, Lei Q, Sirois JE, Bayliss DA (2000) TASK-1, a two-pore domain K^+ channel, is modulated by multiple neurotransmitters in motoneurons. Neuron 25:399–410.

Tang XD, Santarelli LC, Heinemann SH, Hoshi T (2004) Metabolic regulation of potassium channels. Annu Rev Physiol 66:131–159.

Tseng-Crank J, Foster CD, Krause JD, Mertz R, Godinot N, DiChiara TJ, Reinhart PH (1994) Cloning, expression, and distribution of functionally distinct Ca^{2+}-activated K^+ channel isoforms from human brain. Neuron 13:1315–1330.

Vergara C, Latorre R, Marrion NV, Adelman JP (1998) Calcium-activated potassium channels. Curr Opin Neurobiol 8:321–329.

Wei A, Solaro C, Lingle C, Salkoff L (1994) Calcium sensitivity of BK-type KCa channels determined by a separable domain. Neuron 13:671–681.

Yuan A, Dourado M, Butler A, Walton N, Wei A, Salkoff L (2000) SLO-2 a K^+ channel with an unusual Cl-dependence. Nat Neurosci 3:771–779.

Yuan A, Sant CM, Wei A, Wang ZW, Pollak K, Nonet M, Kaczmarek L, Crowder CM, Salkoff L (2003) The sodium-activated potassium channel is encoded by a member of the Slo gene family. Neuron 37:765–773.

Zeng XH, Xia XM, Lingle CJ (2005) Divalent cation sensitivity of BK channel activation supports the existence of three distinct binding sites. J Gen Physiol 125:273–286.